



Coastline, Dili district

Chapter 3

East Timor (Timor-Leste)

The contributions of Terencio Fernandes Moniz and Sebastião da Silva from the National Directorate of Meteorology and Geophysics are gratefully acknowledged

Introduction

This chapter provides a brief description of East Timor, its past and present climate as well as projections for the future. The climate observation network and the availability of atmospheric and oceanic data records are outlined. Seasonal cycles are described and the influences of large-scale climate features (e.g. the South Pacific Convergence Zone) and patterns of climate variability (e.g. the

El Niño-Southern Oscillation) are analysed and discussed. Observed trends and analysis of rainfall, extreme events (including tropical cyclones), sea-surface temperature, ocean acidification, sea level and mean sea level are presented. Projections for air and sea-surface temperature, rainfall, extreme events, ocean acidification and sea level for the 21st century are provided. These projections are

presented along with confidence levels based on expert judgement by Pacific Climate Change Science Program (PCCSP) scientists. The chapter concludes with a summary table of projections (Table 3.3). Important background information, including an explanation of methods and models, is provided in Chapter 1. For definitions of other terms refer to the Glossary.

3.1 Climate Summary

3.1.1 Current Climate

- Dili has a very marked wet season from December to May and a dry season from June to November.
- Sea-surface temperatures are closely related to air temperatures and show a weak seasonal cycle with highest temperatures in March and November, about 2.5°C warmer than those in July, the coolest month.
- Air temperature trends are not presented as there is insufficient data available for the 1950–2009 period.
- Negative trends in annual and dry season rainfall at Dili Airport for the period 1952–2009 are statistically significant.
- The sea-level rise near East Timor measured by satellite altimeters since 1993 is about 9 mm per year.
- On average Dili experiences eight tropical cyclones per decade, with most occurring between November and April, however, the effect is usually weak.

3.1.2 Future Climate

Over the course of the 21st century:

- Surface air temperature and sea-surface temperature are projected to continue to increase (*very high* confidence).
 - Wet season rainfall is projected to increase (*moderate* confidence).
 - Dry season rainfall is projected to decrease (*moderate* confidence).
 - Little change is projected in annual mean rainfall (*low* confidence).
 - The intensity and frequency of days of extreme heat are projected to increase (*very high* confidence).
 - The intensity and frequency of days of extreme rainfall are projected to increase (*high* confidence).
 - Little change is projected in the incidence of drought (*low* confidence).
- Tropical cyclone numbers are projected to decline in the broad region surrounding East Timor (0–20°S and 100°E–130°E) (*moderate* confidence).
 - Ocean acidification is projected to continue (*very high* confidence).
 - Mean sea-level rise is projected to continue (*very high* confidence).

3.2 Country Description

East Timor lies between 8°S–10°S and 124°E–128°E at the eastern end of the Indonesian archipelago. East Timor comprises the eastern half of Timor Island and includes the exclave of Oecusse-Ambeno as well as the two islands, Atauro and Jaco. A mountain range divides the north and south coasts of Timor-Leste. The highest peak is Mount Ramelau (Timor-Leste Country Statistics, 2011).

The population of East Timor in the 2010 census was 1 066 582, most of which live in, or around, the capital of Dili. East Timor's total land area is 15 007 km² which is divided in to 13 administrative districts (Timor-Leste Country Statistics, 2011).

East Timor is a low to middle income economy that continues to suffer the after-effects of decades-long conflict, which damaged infrastructure and displaced thousands of people. Oil and gas deposits are responsible for a large part of East Timor's revenue. Major export commodities include coffee, vanilla, coconut, sandalwood and marble (East Timor Country Brief, 2011).



Figure 3.1: East Timor

3.3 Data Availability

There are currently five operational stations in the East Timor national meteorological network. The primary climate station is located at Dili Airport, near the nation's capital, on the northern side of the island of Timor (Figure 3.1). Rainfall and air temperature data are available for Dili Airport from 1952 and 2003 to present respectively. Observations likely began much earlier; however, these records are yet to be located.

Rainfall data for Dili Airport for 1950–2009 have been used. This record is 90% complete and homogeneous. The available temperature data record is not long enough to provide information about trends in temperature.

There are no tide gauge data available for East Timor, so the Wyndham (Western Australia; since 1984) record has been used as the closest available gauge (Figure 3.8). Both satellite (from 1993) and in situ sea-level data

(1950–2009; termed reconstructed sea level; Volume 1, Section 2.2.2.2) are available on a global $1^\circ \times 1^\circ$ grid.

Long-term locally-monitored sea-surface temperature data are unavailable for East Timor, so large-scale gridded sea-surface temperature datasets have been used (HadISST, HadSST2, ERSST and Kaplan Extended SST V2; Volume 1, Table 2.3).

3.4 Seasonal Cycles

Temperature records from Dili are not long enough to calculate an accurate climatology for the site. Annual variations in sea-surface temperatures near Dili are likely to be closely related to air temperatures, and show a weak seasonal cycle with highest temperatures in March and November, about 2.5°C warmer than those in July, the coolest month.

The seasonal cycle of rainfall (Figure 3.2) shows that Dili has a very marked wet season from December to May and a dry season from June to November. The effect of the West Pacific Monsoon is very strong. For most of the wet season average monthly rainfall is above 100 mm while for most of the dry season it is less than 30 mm. With regards to wind flow, south-east trade winds dominate in Dili, except during the monsoon season when the winds are predominately westerlies. The different phases of the Madden-Julian Oscillation (Volume 1, Section 2.4.4) bring active and dry periods within the monsoon season.

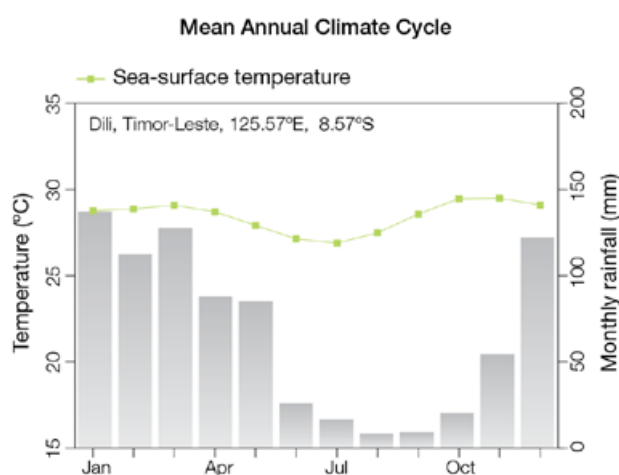


Figure 3.2: Mean annual cycle of rainfall (grey bars) at Dili Airport and local sea-surface temperatures derived from the HadISST dataset (Volume 1, Table 2.3).

3.5 Climate Variability

Due to the short temperature records in Dili, it is not possible to calculate correlation coefficients to determine the impact of large-scale climate variability on temperature. High year-to-year rainfall variability is observed (Figure 3.3). In the dry season there are clear influences on rainfall from a number of components of climate variability, however no significant correlations are found between indicators of this variability in the wet season (Table 3.1). Both the El Niño-Southern Oscillation (ENSO) and the Indian Ocean Dipole (IOD) are related to dry-season rainfall in Dili. El Niño events generally bring drier conditions to Dili, and although they often lead to a late onset and early finish to the wet season, there is no clear influence of ENSO on total wet season rainfall. During La Niña events, dry-season rainfall tends to be above normal, and the wet season often starts earlier and finishes later.

During a positive phase of the IOD, rainfall is lower than normal as seen by the significant correlation between dry season rainfall and the IOD Index (Table 3.1). However, ENSO and IOD are not completely independent. When the relationship between ENSO and the IOD is removed, the correlation

is still significant, but weaker (-0.37). The IOD impact is only seen in the dry season, as the IOD is usually not active in the wet season. ENSO Modoki events (Volume1, Section 3.4.1) also affect dry season rainfall but the relationship is slightly weaker than for canonical ENSO events.

Table 3.1: Correlation coefficients between indices of key large-scale climate variability and minimum and maximum temperatures (Tmin and Tmax) and rainfall at Dili Airport. Only correlation coefficients that are statistically significant at the 95% level are shown.

Climate feature/index		Dry season (June–November)	Wet season (December–May)
		Rain	Rain
ENSO	Niño3.4	-0.52	
	Southern Oscillation Index	0.61	
Interdecadal Pacific Oscillation Index			
Indian Ocean Dipole Index		-0.54	
ENSO Modoki Index		-0.45	
Number of years of data		51	48



Climate data management training, National Directorate of Meteorology and Geophysics

3.6 Observed Trends

3.6.1 Air Temperature

There is insufficient data available to provide air temperature trends from 1950 to 2009. Data is only available from 2003 to 2009.

3.6.2 Rainfall

The Dili Airport negative annual and dry season rainfall trends for the period 1952–2009 are statistically significant. The wet season rainfall trend is not statistically significant (Table 3.2 and Figure 3.3).

Table 3.2: Annual and seasonal trends in rainfall at Dili Airport for the period 1952–2009. Asterisks indicate significance at the 95% level. Persistence is taken into account in the assessment of significance as in Power and Kociuba (in press).

Dili Airport Rain (mm per 10 yrs)	
Annual	-41*
Wet season	+14
Dry season	-26*

3.6.3 Extreme Events

Tropical cyclones can affect East Timor between November and April but their effect has been weak due to East Timor's proximity to the equator. Occurrences outside November to April are rare. The tropical cyclone archive for the Southern Hemisphere indicates that between the 1969/70 and 2009/10 seasons, the centre of 31 tropical cyclones passed within approximately 400 km of Dili (Figure 3.4). This represents an average of eight cyclones per decade. Tropical cyclone occurrences in El Niño, La Niña and neutral years are similar (six, eight and nine cyclones per decade, respectively).

ENSO has a notable effect on East Timor's climate. During La Niña years above-normal rainfall leads

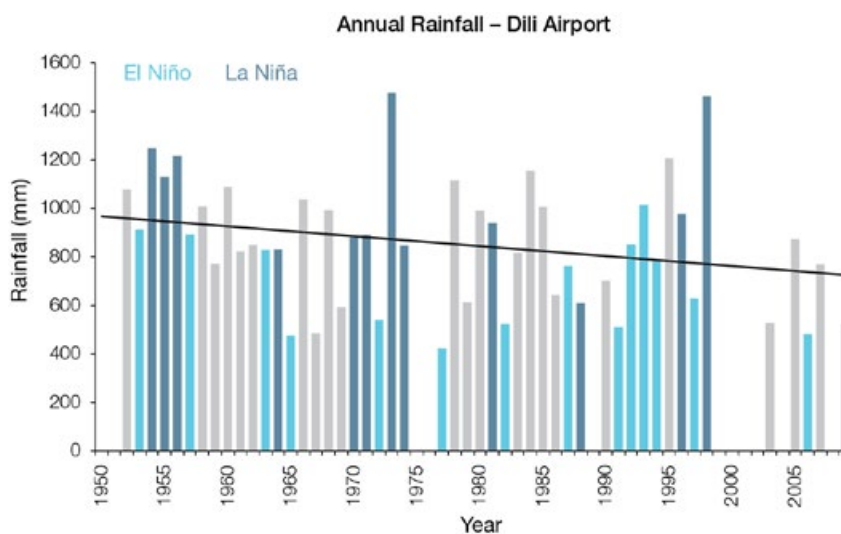


Figure 3.3: Annual rainfall at Dili Airport. Light blue, dark blue and grey bars denote El Niño, La Niña and neutral years respectively.

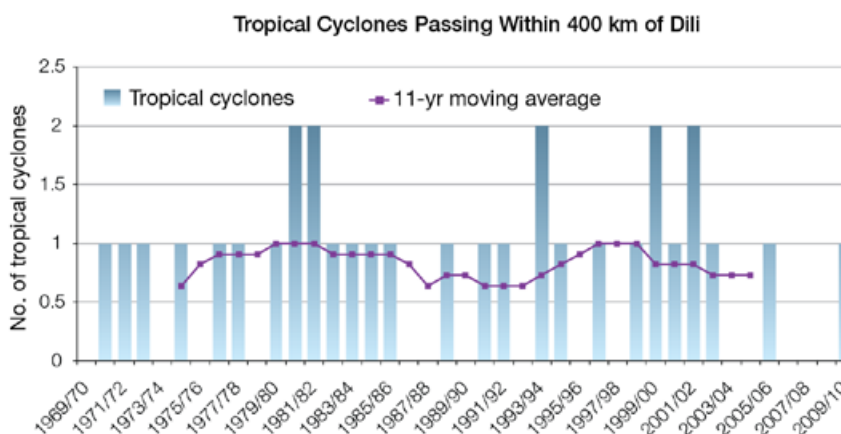


Figure 3.4: Tropical cyclones passing within 400 km of Dili per season. The 11-year moving average is in purple.

to increased frequency of flooding and landslides. El Niño years are associated with droughts. The most significant impact on the population during El Niño years is reduced ground water availability.

3.6.4 Sea-Surface Temperature

Water temperatures around East Timor have risen gradually since the 1950s. Since the 1970s the rate of

warming has been approximately 0.16°C per decade. At these regional scales, natural variability plays a large role in determining the sea-surface temperature, making it difficult to identify long-term trends. Figure 3.6 shows the 1950–2000 sea-surface temperature trends (relative to a reference year of 1990) from different large-scale gridded sea-surface temperature datasets (HadISST, HadSST2, ERSST and Kaplan Extended SST V2; Volume 1, Table 2.3).

3.6.5 Ocean Acidification

No data are available for East Timor.

3.6.6 Sea Level

Monthly averages of the closest available tide gauge (Wyndham, since 1984), satellite (since 1993) and gridded sea-level (since 1950) data agree well and indicate interannual

variability in sea levels of about 24 cm (estimated 5–95% range) after removal of the seasonal cycle (Figure 3.8). The sea-level rise near East Timor, measured by satellite altimeters (Figure 3.5) since 1993, is about 9 mm per year, larger than the global average of 3.2 ± 0.4 mm per year. This rise is partly linked to a pattern related to climate variability from year to year and decade to decade (Figure 3.8).

3.6.7 Extreme Sea-Level Events

This analysis could not be undertaken as there are no tide gauge data available for East Timor.

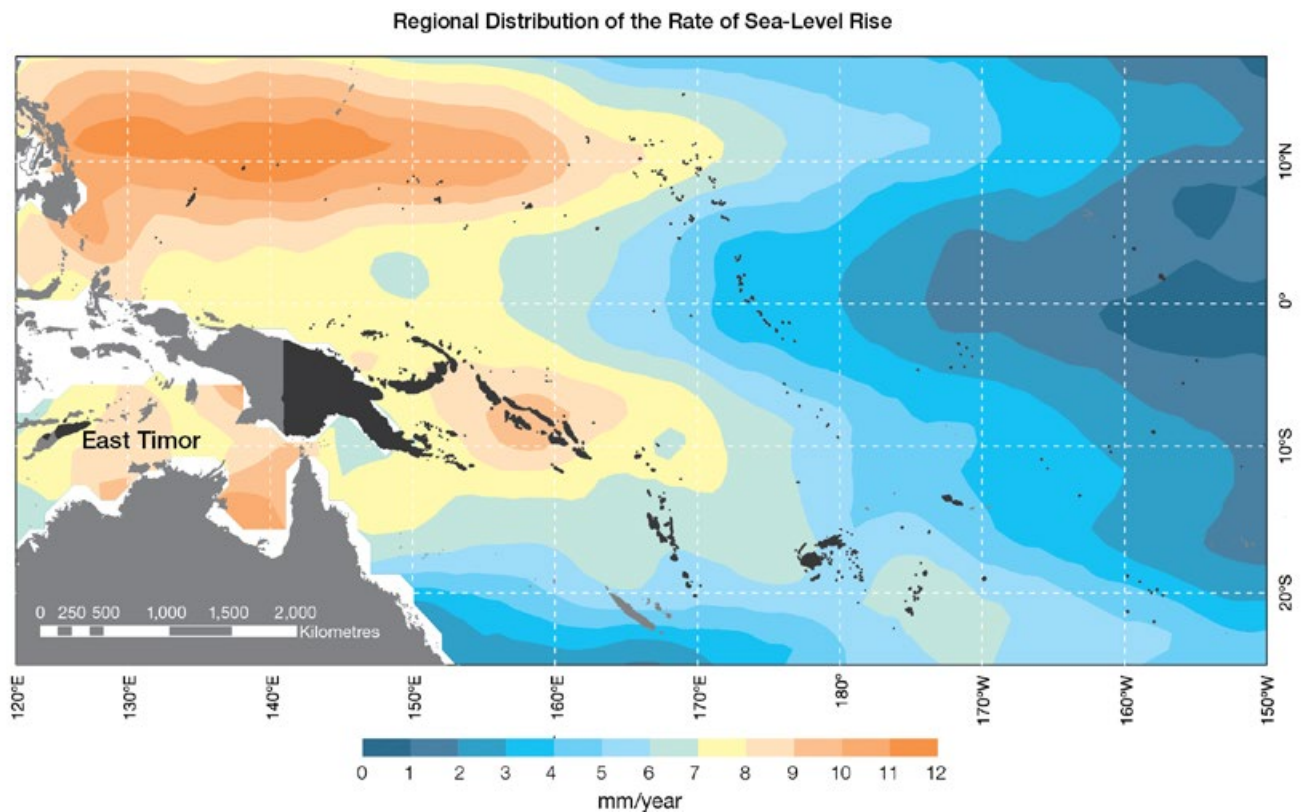


Figure 3.5: The regional distribution of the rate of sea-level rise measured by satellite altimeters from January 1993 to December 2010, with the location of East Timor indicated. Further information on regional distribution of sea-level rise is provided in Volume 1, Section 3.6.3.2.

3.7 Climate Projections

Climate projections have been derived from up to 18 global climate models from the CMIP3 database, for up to three emissions scenarios (B1 (low), A1B (medium) and A2 (high)) and three 20-year periods (centred on 2030, 2055 and 2090, relative to 1990). These models were selected based on their ability to reproduce important features of the current climate (Volume 1, Section 5.2.3), so projections arising from each of the models are a plausible representation of the future climate. This means there is not one single projected future for East Timor, but rather a range of possible futures. The full range of these futures is discussed in the following sections.

These projections do not represent a value specific to any actual location, such as a town or city in East Timor. Instead, they refer to an average change over the broad geographic region encompassing East Timor and the surrounding ocean (Figure 1.1 shows the regional boundaries). Some information regarding dynamical downscaling simulations from the CCAM model (Section 1.7.2) is also provided, in order to indicate how changes in the climate on an individual island-scale may differ from the broad-scale average.

Important information about understanding climate model projections is provided in Section 1.7. A more detailed discussion of East Timor's future climate can also be found in Kirono (2010).

3.7.1 Temperature

Surface air temperature and sea-surface temperature are projected to continue to increase over the course of the 21st century. There is *very high* confidence in this direction of change because:

- Warming is physically consistent with rising greenhouse gas concentrations.
- All CMIP3 models agree on this direction of change.

The majority of CMIP3 models simulate a slight increase (<1°C) in annual and seasonal mean surface air temperature

by 2030, however by 2090 under the A2 (high) emissions scenario increases of greater than 2.5°C are simulated by almost all models (Table 3.3). Given the close relationship between surface air temperature and sea-surface temperature, a similar (or slightly weaker) rate of warming is projected for the surface ocean (Figure 3.6). There is *high* confidence in this range and distribution of possible futures because:

- There is generally close agreement between modelled and observed temperature trends (from reanalysis data) over the past 50 years in the vicinity of East Timor, although observational records are limited (Figure 3.8).

The 8 km CCAM simulations suggest that projected changes in surface air

temperature over land can be up to 1°C greater than over the surrounding ocean. This suggests that the CMIP3 models may slightly underestimate future increases in land temperature. Inland regions are also projected to warm faster than coastal regions.

Interannual variability in surface air temperature and sea surface temperature over East Timor is strongly influenced by ENSO in the current climate (Section 3.5). Projections of future ENSO activity (Volume 1, Section 6.4.1) are not consistent, so it is not possible to determine whether interannual variability in temperature will change in the future. However, ENSO is expected to continue to be an important source of variability for East Timor and the region.

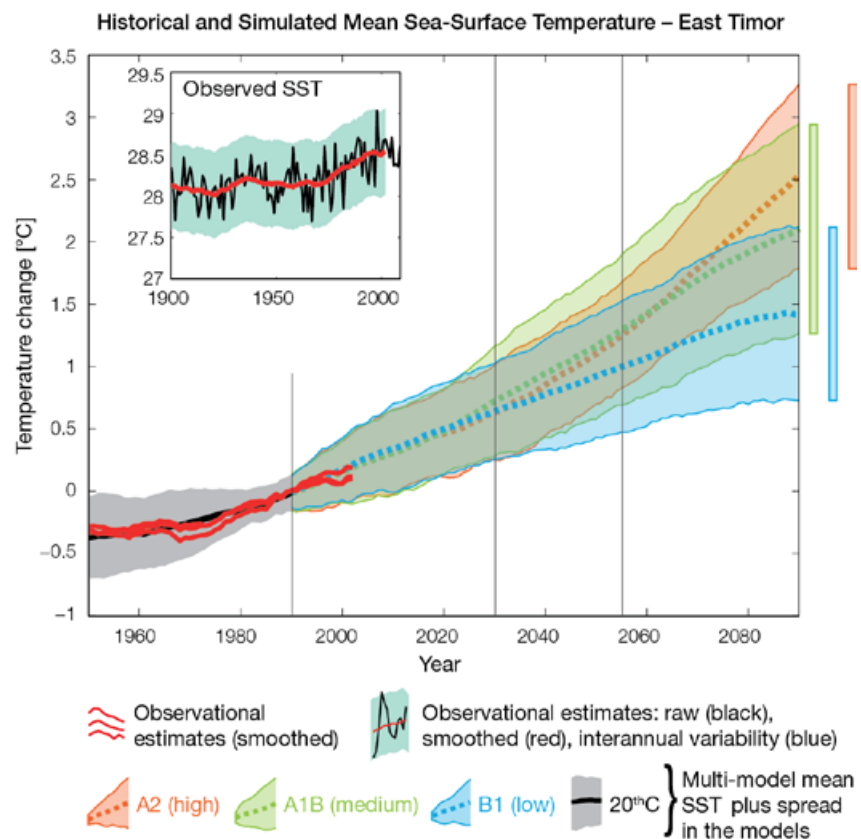


Figure 3.6: Historical climate (from 1950 onwards) and simulated historical and future climate for annual mean sea-surface temperature (SST) in the region surrounding East Timor, for the CMIP3 models. Shading represents approximately 95% of the range of model projections (twice the inter-model standard deviation), while the solid lines represent the smoothed (20-year running average) multi-model mean temperature. Projections are calculated relative to the 1980–1999 period (which is why there is a decline in the inter-model standard deviation around 1990). Observational estimates in the main figure (red lines) are derived from the HadSST2, ERSST and Kaplan Extended SST V2 datasets (Volume 1, Section 2.2.2). Annual average (black) and 20-year running average (red) HadSST2 data is also shown inset.

3.7.2 Rainfall

Wet Season (November-April)

Wet season rainfall is projected to increase over the course of the 21st century. There is *moderate* confidence in this direction of change because:

- An increase in wet season rainfall is consistent with the projected likely amplification of the seasonal rainfall-cycle associated with the West Pacific Monsoon (WPM; Volume 1, Section 6.4.4)
- Approximately half of the CMIP3 models agree on this direction of change by 2090.

The majority of CMIP3 models simulate little change (-5% to 5%) in wet season rainfall by 2030, however by 2090 under the higher emissions scenarios (i.e. A1B (medium) and A2 (high)) the models are approximately equally divided between an increase (>5%) and little change, with only two models suggesting a decline (< -5%) (Table 3.3). There is *moderate* confidence in this range and distribution of possible futures because:

- The majority of CMIP3 models correctly simulate the seasonal cycle of rainfall over East Timor, however the region is subject to large model biases relating to the position of the West Pacific Warm Pool (Volume 1, Section 5.2.2.1).
- The CMIP3 models are unable to resolve many of the physical processes involved in producing rainfall. As a consequence, they do not simulate rainfall as well as other variables such as temperature (Volume 1, Chapter 5).

Dry Season (May-October)

Dry season rainfall is projected to decrease over the course of the 21st century. There is *moderate* confidence in this direction of change because:

- Reduced dry season rainfall is consistent with the projected likely amplification of the seasonal rainfall-cycle associated with the WPM (Volume 1, Section 6.4.4).

- The majority of CMIP3 models agree on this direction of change by 2090.

Approximately half of CMIP3 models simulate little change (-5% to 5%) in dry season rainfall by 2030, however by 2090 under the higher emissions scenarios (i.e. A1B (medium) and A2 (high)) the majority of models simulate a decrease, with the remainder approximately equally divided between a increase (> 5%) and little change (Table 3.3). There is *moderate* confidence in this range and distribution of possible futures because:

- The majority of CMIP3 models correctly simulate the seasonal cycle of rainfall over East Timor, however the region is subject to large model biases relating to the position of the West Pacific Warm Pool (Volume 1, Section 5.2.2.1).
- The CMIP3 models are unable to resolve many of the physical processes involved in producing rainfall.

Annual

Little change is projected in total annual rainfall over the course of the 21st century. There is *low* confidence in this direction of change because:

- Only approximately half of the CMIP3 models suggest this direction of change by 2090.
- There is only moderate confidence in wet and dry season rainfall projections, as discussed.

Interannual variability in rainfall over East Timor is strongly influenced by ENSO in the current climate, via its influence on WPM activity (Section 3.5). As there is no consistency in projections of future ENSO activity (Volume 1, Section 6.4.1), it is not possible to determine whether interannual variability in rainfall will change in the future.

3.7.3 Extremes

Temperature

The intensity and frequency of days of extreme heat are projected to increase over the course of the 21st century. There is *very high* confidence in this direction of change because:

- An increase in the intensity and frequency of days of extreme heat is physically consistent with rising greenhouse gas concentrations.
- All CMIP3 models agree on the direction of change for both intensity and frequency.

The majority of CMIP3 models simulate an increase of approximately 1°C in the temperature experienced on the 1-in-20-year hot day by 2055 under the B1 (low) emissions scenario, with an increase of over 2.5°C simulated by the majority of models by 2090 under the A2 (high) emissions scenario (Table 3.3). There is *low* confidence in this range and distribution of possible futures because:

- In simulations of the current climate, the CMIP3 models tend to underestimate the intensity and frequency of days of extreme heat (Volume 1, Section 5.2.4).
- Smaller increases in the frequency of days of extreme heat are projected by the CCAM 60 km simulations.

Rainfall

The intensity and frequency of days of extreme rainfall are projected to increase over the course of the 21st century. There is *high* confidence in this direction of change because:

- An increase in the frequency and intensity of extreme rainfall is consistent with larger-scale projections, based on the physical argument that the atmosphere is able to hold more water vapour in a warmer climate (Allen and Ingram, 2002; IPCC, 2007). It is also consistent with the projected likely amplification of the seasonal rainfall cycle associated with the WPM (Volume 1, Section 6.4.4).

- Almost all of the CMIP3 models agree on this direction of change for both intensity and frequency.

The majority of CMIP3 models simulate an increase of at least 15 mm in the amount of rain received on the 1-in-20-year wet day by 2055 under a B1 (low) emissions scenario, with an increase of at least 40 mm simulated by all models by 2090 under the A2 (high) emissions scenario. The majority of models project that the current 1-in-20-year extreme rainfall event will occur, on average, four times per 20-year period by 2055 under the B1 (low) emissions scenario and between five and six times per 20-year period by 2090 under the A2 (high) emissions scenario. There is *low* confidence in this range and distribution of possible futures because:

- In simulations of the current climate, the CMIP3 models tend to underestimate the intensity and frequency of extreme rainfall (Volume 1, Section 5.2.4).
- The CMIP3 models are unable to resolve many of the physical processes involved in producing extreme rainfall.

Drought

Little change is projected in the incidence of drought over the course of the 21st century. There is *low* confidence in this direction of change because:

- There is only low confidence in annual rainfall projections (Section 3.7.2), which directly influences projections of future drought conditions.

The majority of CMIP3 models project that mild drought will occur approximately 8–10 times every 20 years across all time periods and emissions scenarios. Moderate drought is projected to occur approximately once to twice every

20 years for all time periods under the A1B (medium) and A2 (high) emissions scenarios, while under the B1 (low) emissions scenario a frequency of two to three times every 20 years is projected by the majority of models for 2030, decreasing to once to twice by 2090. The majority of CMIP3 models project that severe droughts will occur approximately once every 20 years across all time periods and emissions scenarios.

Tropical Cyclones

Tropical cyclone numbers are projected decline for the broad region surrounding East Timor (0–20°S, 100°E–130°E) over the course of the 21st century. There is *moderate* confidence in this direction of change because:

- Many studies suggest a decline in tropical cyclone frequency globally (Knutson et al., 2010).
- Tropical cyclone numbers decline in the East Timor region in the majority of PCCSP assessment techniques.

Projected changes based on the direct detection methodologies (Curvature Vorticity Parameter (CVP) and the CSIRO Direct Detection Scheme (CDD); Volume 1, Section 4.8.2), indicate a decrease in tropical cyclone formation. When these techniques are applied to CCAM, 100% of projections show a decrease in tropical cyclone formation. In addition, the Genesis Potential Index (GPI) empirical technique suggests that conditions for tropical cyclone formation will become less favourable in the East Timor region for almost all analysed CMIP3 models. There is *moderate* confidence in this projection because in simulations of the current climate, the CVP, CDD and GPI methods capture the frequency of tropical cyclone activity reasonably well (Volume 1, Section 5.4).

3.7.4 Ocean Acidification

Aragonite saturation states above about 4 are considered optimal for coral growth and for the development of healthy reef ecosystems. While values between 3.5 and 4 are considered adequate, values between 3 and 3.5 are considered marginal, while values below 3 are considered extremely marginal (Guinotte et al., 2003).

The acidification of the ocean will continue to increase over the course of the 21st century. There is *very high* confidence in this projection as the rate of ocean acidification is driven primarily by the increasing oceanic uptake of carbon dioxide, in response to rising atmospheric carbon dioxide concentrations.

Projections from all analysed CMIP3 models indicate that the annual maximum aragonite saturation state will reach values below 3.5 by about 2025 and continue to decline thereafter (Figure 3.7; Table 3.3). There is *moderate* confidence in this range and distribution of possible futures because the projections are based on climate models without an explicit representation of the carbon cycle and with relatively low resolution and known regional biases.

The impact of acidification change on the health of reef ecosystems is likely to be compounded by other stressors including coral bleaching, storm damage and fishing pressure.

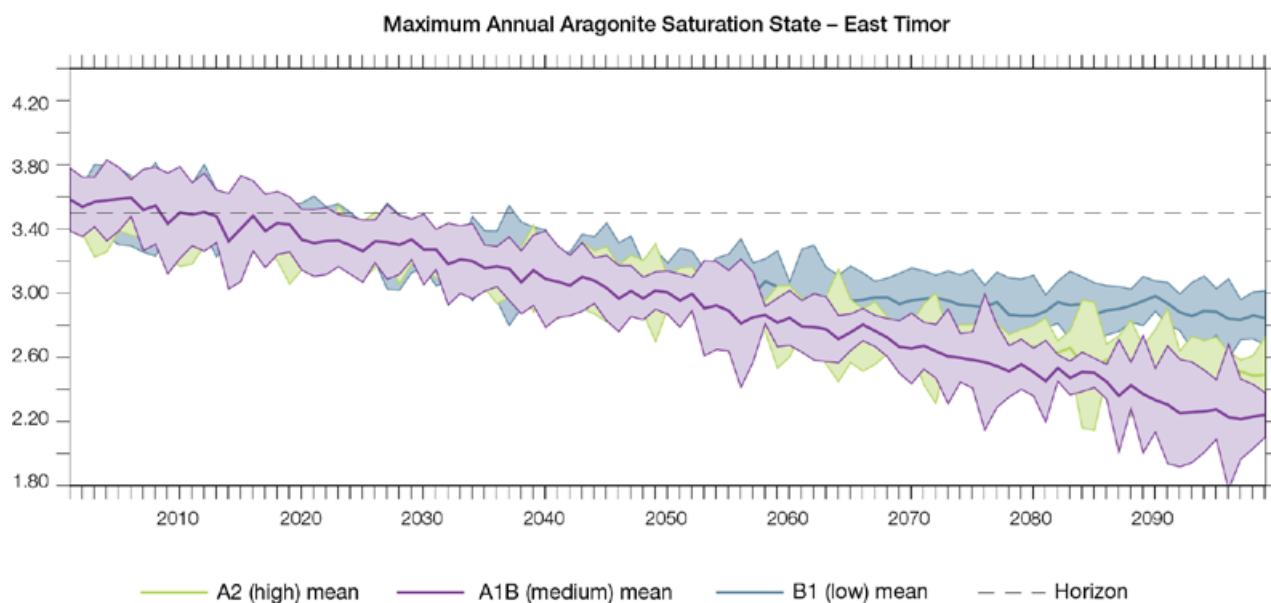


Figure 3.7: Multi-model projections, and their associated uncertainty (shaded area represents two standard deviations), of the maximum annual aragonite saturation state in the sea surface waters of the East Timor region under the different emissions scenarios. The dashed black line represents an aragonite saturation state of 3.5.

3.7.5 Sea Level

Mean sea level is projected to continue to rise over the course of the 21st century. There is *very high* confidence in this direction of change because:

- Sea-level rise is a physically consistent response to increasing ocean and atmospheric temperatures, due to thermal expansion and the melting of glaciers and ice caps.
- Projections from all CMIP3 models agree on this direction of change.

The CMIP3 models simulate a rise of between approximately 5–15 cm by 2030, with increases of 20–60 cm indicated by 2090 under the higher emissions scenarios (i.e. A1B (medium) and A2 (high); Figure 3.8; Table 3.3).

There is *moderate* confidence in this range and distribution of possible futures because:

- There is significant uncertainty surrounding ice-sheet contributions to sea-level rise and a rise larger than projected above cannot be excluded (Meehl et al., 2007b). However, understanding of the processes is currently too limited to provide a best estimate or an upper bound (IPCC, 2007).
- Globally, since the early 1990s, sea level has been rising near the upper end of the above projections. During the 21st century, some studies (using semi-empirical models) project faster rates of sea-level rise.

Interannual variability of sea level will lead to periods of lower and higher regional sea levels. In the past, this interannual variability has been about 24 cm (5–95% range, after removal of the seasonal signal; dashed lines in Figure 3.8 (a)) and it is likely that a similar range will continue through the 21st century. In addition, winds and waves associated with weather phenomena will continue to lead to extreme sea-level events.

In addition to the regional variations in sea level associated with ocean and mass changes, there are ongoing changes in relative sea level associated with changes in surface loading over the last glacial cycle (glacial isostatic adjustment) and local tectonic motions. The glacial isostatic motions are relatively small for the PCCSP region.

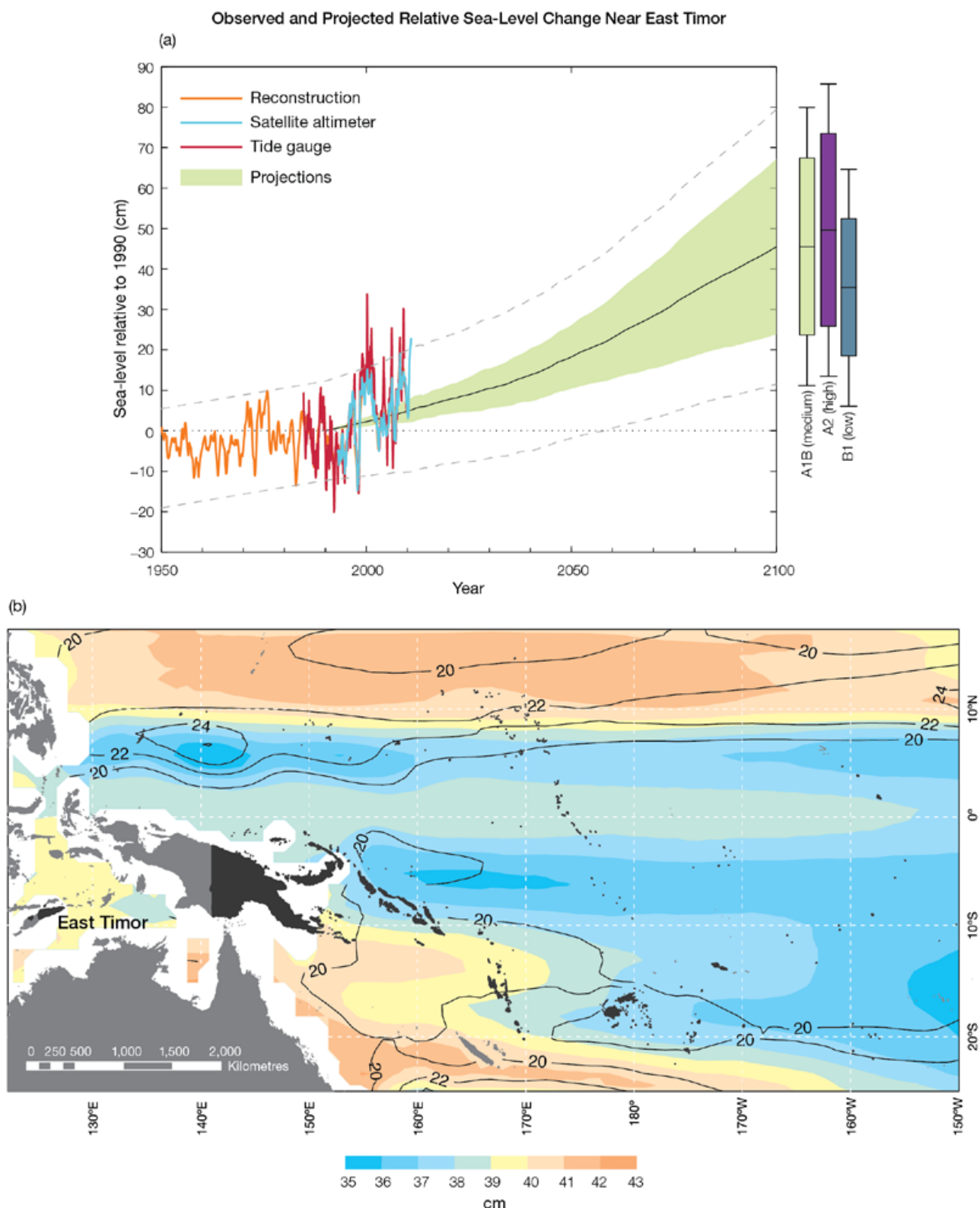


Figure 3.8: Observed and projected relative sea-level change near East Timor. (a) The observed in situ relative sea-level records from the closest available gauge at Wyndham are indicated in red, with the satellite record (since 1993) in light blue. The gridded sea level at East Timor (since 1950, from Church and White (in press)) is shown in orange. The projections for the A1B (medium) emissions scenario (5–95% uncertainty range) are shown by the green shaded region from 1990–2100. The range of projections for the B1 (low), A1B (medium) and A2 (high) emissions scenarios are also shown by the bars on the right. The dashed lines are an estimate of interannual variability in sea level (5–95% range about the long-term trends) and indicate that individual monthly averages of sea level can be above or below longer-term averages. (b) The projections (in cm) for the A1B (medium) emissions scenario in the East Timor region for the average over 2081–2100 relative to 1981–2000 are indicated by the shading, with the estimated uncertainty in the projections indicated by the contours (in cm).

3.7.6 Projections Summary

The projections presented in Section 3.7 are summarised in Table 3.3. For detailed information regarding the various uncertainties associated with the table values, refer to the preceding text in Sections 3.7 and 1.7, in addition to Chapters 5 and 6 in Volume 1. When interpreting the differences between projections for the B1 (low), A1B (medium) and A2 (high) emissions scenarios, it is also important to consider the emissions pathways associated with each scenario (Volume 1, Figure 4.1) and the fact that a slightly different subset of models was available for each (Volume 1, Appendix 1).

Table 3.3: Projected change in the annual and seasonal mean climate for East Timor, under the B1 (low; blue), A1B (medium; green) and A2 (high; purple) emissions scenarios. Projections are given for three 20-year periods centred on 2030 (2020–2039), 2055 (2046–2065) and 2090 (2080–2099), relative to 1990 (1980–1999). Values represent the multi-model mean change \pm twice the inter-model standard deviation (representing approximately 95% of the range of model projections), except for sea level where the estimated mean change and the 5–95% range are given (as they are derived directly from the Intergovernmental Panel on Climate Change Fourth Assessment Report values). The confidence (Section 1.7.2) associated with the range and distribution of the projections is also given (indicated by the standard deviation and multi-model mean, respectively). See Volume 1, Appendix 1, for a complete listing of CMIP3 models used to derive these projections.

Variable	Season	2030	2055	2090	Confidence
Surface air temperature (°C)	Annual	+0.7 \pm 0.4	+1.1 \pm 0.6	+1.5 \pm 0.7	High
		+0.8 \pm 0.4	+1.5 \pm 0.6	+2.3 \pm 0.9	
		+0.7 \pm 0.3	+1.4 \pm 0.4	+2.8 \pm 0.7	
Maximum temperature (°C)	1-in-20-year event	N/A	+1.0 \pm 0.6	+1.4 \pm 0.8	Low
			+1.4 \pm 0.6	+2.2 \pm 1.1	
			+1.5 \pm 0.5	+2.8 \pm 1.5	
Minimum temperature (°C)	1-in-20-year event	N/A	+1.3 \pm 1.6	+1.7 \pm 1.6	Low
			+1.6 \pm 1.8	+2.2 \pm 1.8	
			+1.6 \pm 1.7	+2.5 \pm 1.8	
Total rainfall (%)*	Annual	+1 \pm 9	0 \pm 15	0 \pm 13	Low
		+1 \pm 8	-1 \pm 18	0 \pm 19	
		0 \pm 11	0 \pm 16	+1 \pm 23	
Wet season rainfall (%)*	November-April	+1 \pm 7	+1 \pm 10	+2 \pm 9	Moderate
		+1 \pm 7	+1 \pm 14	+2 \pm 15	
		0 \pm 8	+3 \pm 10	+5 \pm 16	
Dry season rainfall (%)*	May-October	+1 \pm 20	-2 \pm 31	-4 \pm 28	Moderate
		+3 \pm 18	-4 \pm 35	-3 \pm 40	
		0 \pm 23	-3 \pm 31	-4 \pm 51	
Sea-surface temperature (°C)	Annual	+0.6 \pm 0.4	+1.0 \pm 0.5	+1.4 \pm 0.7	High
		+0.7 \pm 0.4	+1.3 \pm 0.6	+2.1 \pm 0.8	
		+0.6 \pm 0.4	+1.2 \pm 0.4	+2.5 \pm 0.7	
Aragonite saturation state (Ω_{ar})	Annual maximum	+3.3 \pm 0.2	+3.0 \pm 0.2	+2.8 \pm 0.2	Moderate
		+3.2 \pm 0.1	+2.9 \pm 0.2	+2.5 \pm 0.2	
		+3.2 \pm 0.2	+2.8 \pm 0.2	+2.3 \pm 0.2	
Mean sea level (cm)	Annual	+10 (6–15)	+18 (10–27)	+32 (17–47)	Moderate
		+11 (6–15)	+21 (12–30)	+40 (21–59)	
		+10 (6–15)	+20 (12–29)	+42 (22–62)	

*The MIROC3.2 (medres) model was eliminated in calculating the rainfall projections, due to its inability to accurately simulate present-day activity of the West Pacific Monsoon (Volume 1, Section 5.5.1).